ACS APPLIED MATERIALS & INTERFACES

Letter

www.acsami.org

Switchable Micropatterned Surface Topographies Mediated by Reversible Shape Memory

Sara A. Turner, Jing Zhou, Sergei S. Sheiko, and Valerie Sheares Ashby*

Department of Chemistry, University of North Carolina, 131 South Road, Chapel Hill, North Carolina 27599, United States

Supporting Information

ABSTRACT: Reversibly switching topography on micrometer length scales greatly expands the functionality of stimuli-responsive substrates. Here we report the first usage of reversible shape memory for the actuation of two-way transitions between microscopically patterned substrates, resulting in corresponding modulations of the wetting properties. Reversible switching of the surface topography is achieved through partial melting and recrystallization of a semi-crystalline polyester embossed with microscopic features. This behavior is monitored with atomic force microscopy (AFM) and contact angle measurements. We demonstrate that the magnitude of the contact angle variations depends on the embossment pattern.

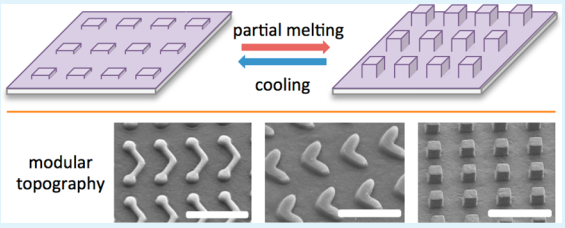

KEYWORDS: *microstructured surfaces, reversible shape memory, topological structure change, responsive surfaces, surface topography*

Nature has produced a number of surfaces that utilize a microstructured topography as a part of their function—the lotus leaf is endowed with a multilayered topography that provides it with superhydrophobicity and thus self-cleaning capabilities,[1] and gecko footpads feature small bristle-like structures, which aid in adhesion and allow these animals to scale smooth vertical surfaces quickly.[2] There are countless reports of synthetic surfaces with physical properties influenced by microstructure topography,[3−6] including adhesion, wetting,[7,8] optical diffraction, and propulsion effects.[9,10] Of particular interest are dynamic surfaces capable of transitioning between two or more physically distinct states due to topographical changes. Liquid crystalline elastomers, lower critical solution temperature polymers, and photoisomerizing materials responding to electrical, thermal, optical, and mechanical stimuli have all been reported for accessing reversibly switching surfaces.[11−15] Shape memory surfaces have also been reported to switch from one surface topography to another. Some distinct advantages of the shape memory process are the ability to program complex shapes,[16,17] its applicability to many length scales (from the nano- to macroscales),[18,19] and its compatibility with well-defined arrays of topographic features with long-range ordering.[5,20] However, a given transition can only occur once before a reprogramming event is necessary.[21,22] Recently, universal principles for enabling truly reversible shape memory (RSM) actuation between distinct shapes in macroscopic semi-crystalline elastomers have been reported.[23,24] We have shown that this widely applicable behavior results from the interplay between a crystalline network and a network of chemical crosslinks, each capable of encoding a distinct shape. In this method, reversibility is achieved through the controlled, partial melting of a crystalline sub-network, resulting in partial recovery of the original shape while maintaining memory of a temporary shape. By controlling the crosslinking density, we have attained ca. 70% reversibility of the original strain. A distinct advantage to the RSM process is that it requires no reprogramming steps between actuation events and can be applied to conventional semi-crystalline elastomers. Furthermore, the observed behavior is repeatable over multiple actuation cycles without applying any external force.

Herein, we report the first instance of reversibly changing macroscopic surface properties via topography switches modulated by RSM. We utilize the thermosetting copolyester poly(octylene adipate)-*co*-poly(octylene diazoadipate) (POAOD)[25] as a representative semicrystalline polymer to fabricate surfaces capable of RSM behavior, and examine microscopic reversible changes in substrate topography via AFM and SEM in addition to changes in macroscopic wetting behavior. Furthermore, we report that these surface changes are reversible, and that the magnitude of a RSM surface switch can be tuned with surface pattern selection.

RSM is a phenomenon derived from the conventional thermal shape memory (SM) of semicrystalline polymers, and employs the same two-step programming protocol to prepare samples for actuation. First, a thermosetting semicrystalline polymer is cured in a mold, which results in the formation of a specific shape secured by a dual network of covalent crosslinks and crystallites. Second, this equilibrium shape is changed by heating to a temperature above the melting transition of the crystallites, applying a deformation, and then quenching to a temperature below the crystallization transition. This results in a metastable shape, wherein the strained conformation of the chemical network is held by a percolated scaffold of crystallites

Received: March 31, 2014
Accepted: May 13, 2014
Published: May 13, 2014

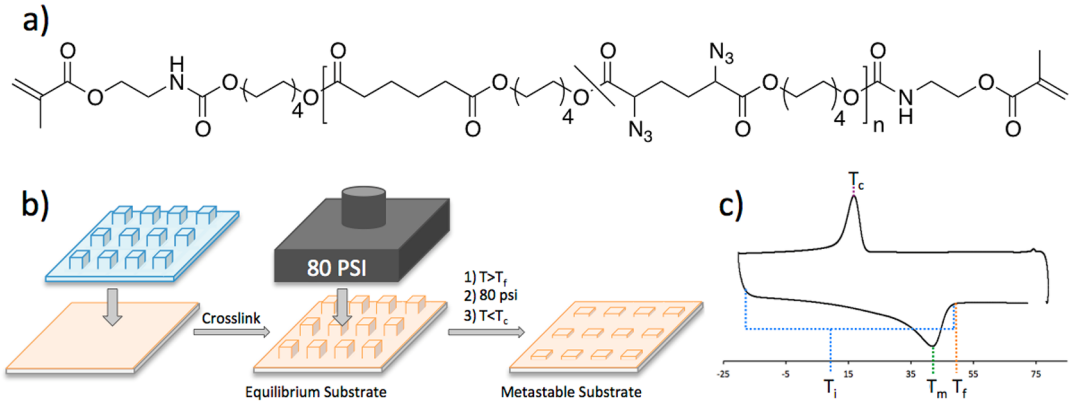

Figure 1. (a) Thermosetting copolyester poly(octylene adipate)-*co*-poly(octylene diazoadipate) (POAOD) has been used for the preparation of semi-crystalline elastomers with a tunable melting temperature.[25] (b) Shape programming process consists of two steps: (i) embossing of a substrate with equilibrium surface topography and (ii) uniaxial compression at an elevated temperature followed by quenching to a metastable shape. (c) DSC thermogram of a characteristic sample of $POAOD_{17:83}$ labeled with T_c = crystallization temperature; T_f = temperature at which all melting is completed; T_m = melting transition peak, traditionally reported as the melting temperature; T_i = a range indicating intermediate melting temperatures.

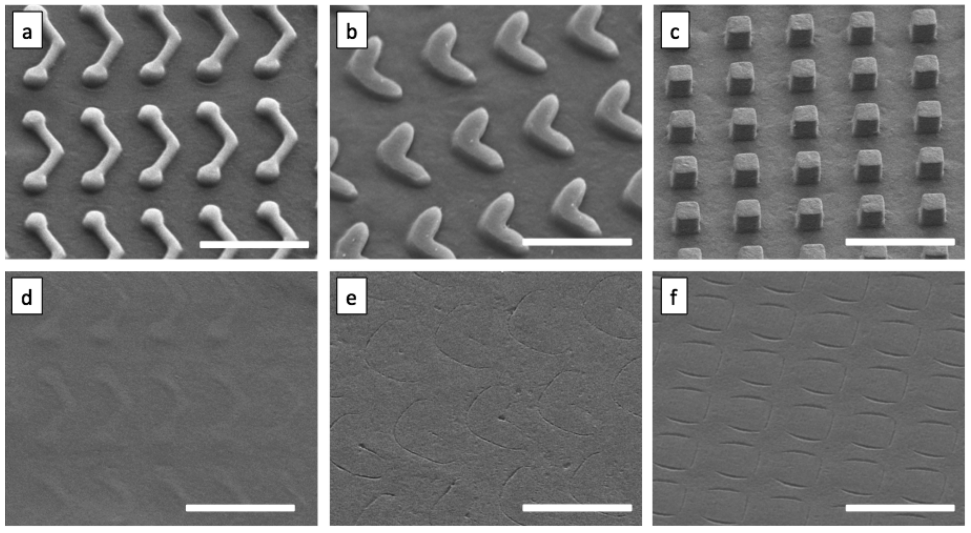

Figure 2. SEM images of surfaces embossed with (a) boomerangs, (b) elbows, and (c) cubes in their equilibrium states, and (d–f) the same surfaces after programming into their metastable states. Surfaces viewed at a 45° tilt. Scale bars are 10 μm.

even after the external force is removed. Figure 1 shows an oversimplified fabrication scheme using particle replication in non-wetting templates (PRINT) molds to fabricate substrates with a range of high fidelity embossed topographies.[26] For this purpose, a solution of poly(octylene adipate)-*co*-poly(octylene diazoadipate) with terminal methacrylate groups (Figure 1a) is crosslinked into a thermoset via radical crosslinking under UV light inside a mold (Figure 1b) yielding an equilibrium substrate with well-defined topography. The equilibrium nature of this topography was ensured by annealing at an elevated temperature above the melting transition. To produce a metastable shape, the substrate was heated to T = 70 °C ($T > T_f$) and compressed by applying an external pressure of 80 psi. This flattened shape was secured by quenching to $T < T_c$ and crystallizing under pressure (Figure 1c). The resulting metastable substrate is primed for either conventional SM or RSM.

Conventional SM of embossed substrates has been explored by our group and by others.[9,22,24,27] Here, we show that RSM of surfaces can be applied to a wide array of surface embossment patterns and enable reversible switching of surface topographies. Because macroscopic surface properties depend on the surface pattern, three unique topographies were chosen for extensive investigation: boomerangs, elbows, and cubes. These topographies were chosen due to their relative ease of fabrication compared to others. Figure 2 shows SEM images of equilibrium (Figure 2a–c) and metastable (Figure 2d–f) substrates after these embossing and compressing steps, respectively. Conventional SM requires that a sample be heated to $T > T_f$ (shown schematically in Figure 1b), the temperature at which all crystallites have melted. But RSM demands partial melting to $T = T_i$, an intermediate melting temperature between the onset and completion of melting.[23] At this intermediate temperature, the crystallites securing the metastable shape begin to melt and destroy percolation of the crystalline scaffold, permitting the polymer network to relax towards its thermodynamically preferred configuration. This process of limited melting results in a partial recovery of the equilibrium shape. In a semi-molten state, both the remaining lamellae and the amorphous strands are fairly constrained

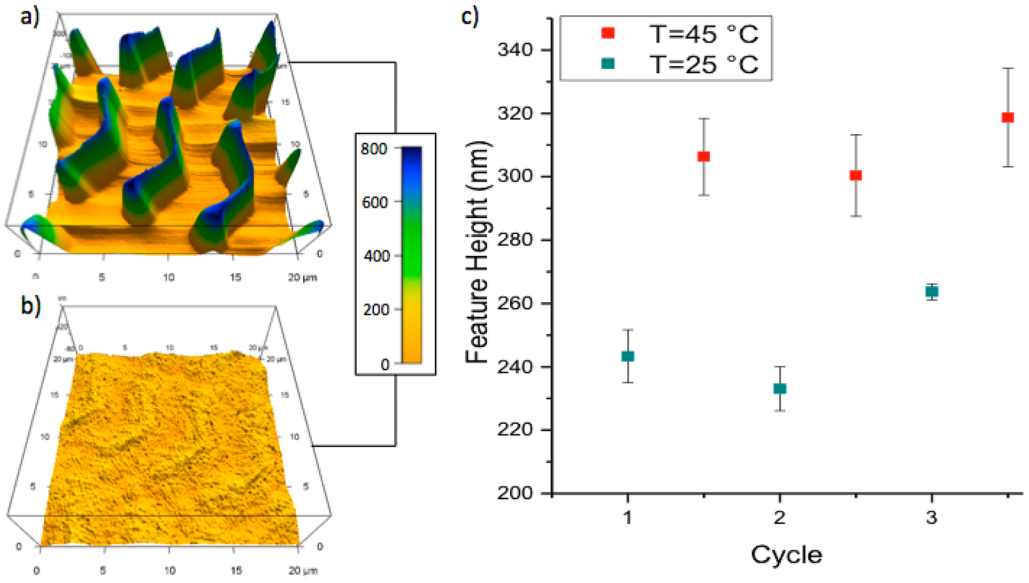

Figure 3. AFM images of boomerang substrates in their (a) equilibrium textured and (b) metastable flat topographies. Height scale is in nanometers. (c) For a given T_i = 45 °C, elongation and compression of boomerang features is shown to be reversible over multiple heating and cooling cycles.

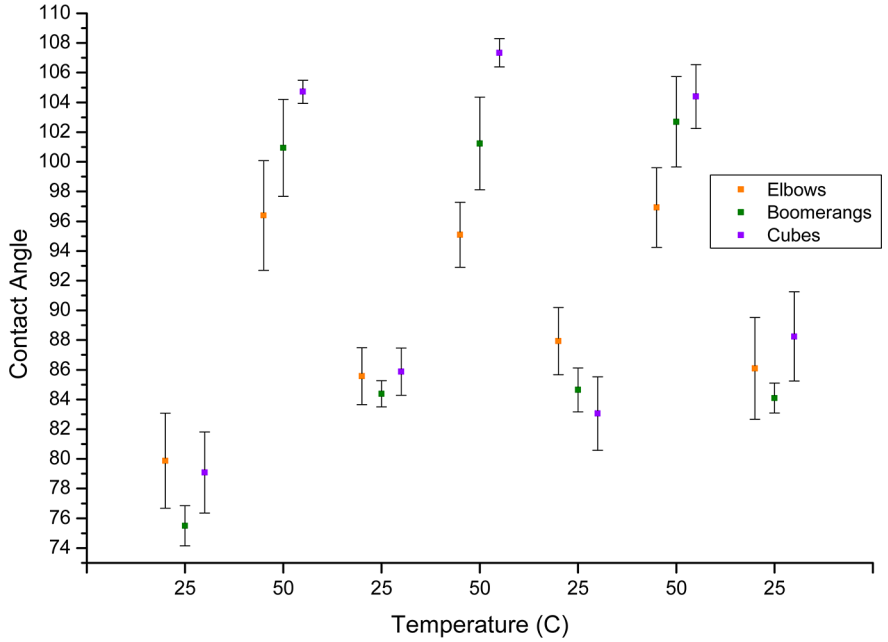

Figure 4. GCAs of the embossed substrates ($POAOD_{10:90}$, T_m = 53 °C) are reversibly modulated by repeated heating and cooling between T = 25 °C and T = 50 °C. All GCAs are measured at t = 15 s after deposition.

within the polymer network, which ensures recrystallization of the crystalline scaffold in their previous position. This process pulls the network back into the same entropically strained state in which it was previously, resulting in partial restoration of the metastable shape. The extent of reversibility (fraction of reversible strain) can be adjusted by controlling the crosslink density and intermediate melting temperature.[23] Furthermore, the melting transition of a POAOD substrate can be tuned by varying the copolymer ratio of octylene adipate and octylene diazoadipate segments.[24] Incorporating a higher proportion of the former monomer increases the size and number of crystalline regions within the polymer network, and thus shifts the melting transition towards higher temperatures. The ability to modulate the melting transition for a given application is an important advantage of the RSM method.

As such, RSM allows for a programmed substrate to transition between physically distinct surfaces with repeated partial melting and recrystallization steps. We utilized AFM to quantify these surface changes. $POAOD_{17:83}$ (T_m = 42 °C) was employed to generate a boomerang substrate primed for RSM. The boomerang topography was chosen for characterization because of its relatively low aspect ratio and the large spacing between features, both of which are favorable for quantitative analysis of the surface topography by AFM. Initial micrographs confirm the significant difference in height between the equilibrium and metastable topographies (Figure 3); in the given 20 × 20 μm^2 window, the features in their equilibrium

dx.doi.org/10.1021/am501970d | ACS Appl. Mater. Interfaces 2014, 6, 8017−8021

state are 669 ± 3 nm and the same features in their programmed metastable state are 88 ± 3 nm in height.

As a metastable boomerang substrate is heated to an intermediate temperature of T_i = 43°C, partial melting of the crystalline scaffold permits the polymer network to relax back towards its equilibrium state, and thus the features increase in height. Subsequent cooling from T_i results in templated recrystallization and reversion towards the metastable state, and the features again decrease in height. Maximizing the difference between the equilibrium and metastable heights, and thus maximizing reversibility overall, is a matter of interplay between the crosslinking network and crystalline scaffold. On the one hand, enough crystalline lamellae must melt in order to allow for a significant change toward the equilibrium state; but on the other hand, a significant fraction of the crystalline scaffold must also remain in order to enable and guide prompt return towards the metastable state upon recrystallization. Therefore, the extent of feature height modulation that is possible with surface RSM is dependent on the identity of T_i. The maximum extent of reversibility is observed at T_i = 45 ± 1 °C, which is slightly above the peak of the melting transition T_m = 42 °C of $POAOD_{17:83}$ (see Figure S1 in the Supporting Information). In Figure 3c, we show that the RSM of this boomerang substrate is repeatable over multiple heating and cooling cycles to T_i = 45 °C. In previous work, we have found that recovery of the metastable state declines slightly (~10% over the first three cycles), but upon further cycling it remains consistent.[23] Thus, the slight degradation of reversibility in the third cycle shown here is consistent with previous research in reversible shape memory.

The ability to modulate surface properties via topography is useful for a variety of potential applications, including actuators,[28] tissue engineering,[29] and microfluidics.[30] To illustrate the tunability of wetting via surface RSM, static contact angle data utilizing glycerol as the liquid phase are provided in Figure 4 for each of the topographies ($POAOD_{10:90}$, T_m = 53 °C) undergoing RSM cycles. The elevated temperatures utilized to acquire this data necessitate a high-boiling liquid for the sessile drop to avoid solvent evaporation. The high boiling point of glycerol (290 °C) and its similar surface energy to water make it an ideal substitute for these contact angle measurements at elevated temperatures.[31]

Each topography in its programmed metastable state displays 75° < glycerol contact angle (GCA) < 80° at t = 15 seconds after drop deposition. The similarity in the wetting behavior of each of these substrates is appropriate considering that each topography almost completely flattened, as is apparent in Figure 2d-f. Upon heating to T_i = 50 °C, the elbow substrate displays a modest wetting change (GCA = 96°) as the topography decompresses in a partial recovery of the equilibrium state. The boomerang substrate changes more significantly (GCA = 102°) upon heating to the same temperature. Finally, we show that the cubic topography changes the most significantly upon heating to T_i (GCA = 105°), consistent with the greater inherent roughness of that topography (see Table S1 in the Supporting Information). Cooling each topography to T = 20 °C results in 83° < GCA < 88°, representing a return toward the flattened metastable topography. We conjecture that the differences among the GCAs at T_i occur because those topographies differ significantly from each other, whereas after cooling they all return to a more flattened, compressed topography, which is similar to all of them. The original GCAs of the programmed metastable state are not fully recovered upon cooling, indicating that the flattened topographies as they appear in Figure 2d–f never reflatten completely; however, the GCA data of each of the two subsequent heating and cooling cycles show that iterative transitions towards the metastable and equilibrium states are repeatable over multiple cycles. These results also demonstrate the tunability of RSM, as we can produce wetting switches of different magnitudes simply by varying the embossment pattern.

We have shown that reversible shape memory, a technique previously only investigated in macroscale objects, is feasible and effective for topographic transformations on the microscale. Using widely accepted soft lithography techniques to pattern a semi-crystalline elastomer with microscale features provides the means to access substrates with switchable topographies upon reversible actuation of the features. We have shown that it is possible to modulate surface wetting by cycling between equilibrium and metastable topographies, and that wetting differences can be modulated with topography. Furthermore, although the pendant azide groups of the polymer backbone were not utilized in this work, their inclusion allows for postfunctionalization of a surface with various alkyne functional groups, permitting further substrate tunability. Because RSM is accessible with any semicrystalline polymer with a broad melting transition, this technique may prove to be broadly applicable for a number of applications requiring different materials, and in particular for applications requiring modular roughness, wetting, or adhesion.

■ ASSOCIATED CONTENT

Supporting Information

Synthesis and characterization data, and contact angle equilibration data for glycerol on equilibrium and metastable boomerang surfaces. This material is available free of charge via the Internet at http://pubs.acs.org.

■ AUTHOR INFORMATION

Corresponding Author

*E-mail: ashby@email.unc.edu.

Funding

This research was supported by NSF DMR-1122483 and NSF Biomaterials DMR-1206957.

Notes

The authors declare no competing financial interest.

■ ACKNOWLEDGMENTS

We thank the DeSimone group for providing expertise and PRINT molds and Dr. Carrie Donley of UNC CHANL for assistance with AFM measurements.

■ REFERENCES

(1) Sun, T.; Feng, L.; Gao, X.; Jiang, L. Bioinspired Surfaces with Special Wettability. *Acc. Chem. Res.* **2005**, *38*, 644–652.

(2) Autumn, K.; Liang, Y. A.; Hsieh, S. T.; Zesch, W.; Chan, W. P.; Kenny, T. W.; Fearing, R.; Full, R. J. Adhesive Force of a Single Gecko Foot-Hair. *Nature* **2000**, *405*, 681–686.

(3) Li, J.; Shim, J.; Deng, J.; Overvelde, J. T. B.; Zhu, X.; Bertoldi, K.; Yang, S. Switching Periodic Membranes via Pattern Transformation and Shape Memory Effect. *Soft Matter* **2012**, *8*, 10322–10328.

(4) Geim, A. K.; Dubonos, S. V.; Grigorieva, I. V.; Novoselov, D. S.; Zhukov, A. A.; Shaproval, S. Y. Microfabricated Adhesive Mimicking Gecko Foot-Hair. *Nat. Mater.* **2003**, *2*, 461–463.

(5) Ebara, M.; Uto, K.; Idota, N.; Hoffman, J.M.; Aoyagi, T. Shape-Memory Surface with Dynamically Tunable Nano-Geometry Activated by Body Heat. *Adv. Mater.* **2012**, *24*, 273−278.
(6) Lee, H.; Lee, B. P.; Lessersmith, P. B. A Reversible Wet/Dry Adhesive Inspired by Mussels and Geckos. *Nature* **2007**, *448*, 338−341.
(7) Persson, B. N. J.; Albohr, O.; Tartaglino, U.; Volokitin, A. I.; Tosatti, E. On the Nature of Surface Roughness with Application to Contact Mechanics, Sealing, Rubber Friction and Adhesion. *J. Phys.: Condens. Matter* **2005**, *17*, R1−R62.
(8) Peressadko, A.G.; Hosoda, N.; Persson, B. N. J. Influence of Surface Roughness on Adhesion between Elastic Bodies. *Phys. Rev. Lett.* **2005**, *95*, 124301/1−124301/4.
(9) Vukusic, P.; Sambles, J. R. Photonic Structures in Biology. *Nature* **2003**, *424*, 852−855.
(10) Dreyfus, R.; Baudry, J.; Roper, M. L.; Fermigier, M.; Stone, H. A.; Bibette, J. Microscopic Artificial Swimmers. *Nature* **2005**, *437*, 862−865.
(11) De Crevoisier, G.; Fabre, P.; Corpart, J.-M.; Leibler, L. Switchable Tackiness and Wettability of a Liquid Crystalline Polymer. *Science* **1999**, *285*, 1246−1249.
(12) Sun, T.; Wang, G.; Feng, L.; Liu, B.; Ma, Y.; Jiang, L.; Zhu, D. Reversible Switching Between Superhydrophilicity and Superhydrophobicity. *Angew. Chem., Int. Ed.* **2004**, *43*, 357−360.
(13) Wu, Z. L.; Wei, R.; Buguin, A.; Taulemesse, J.-M.; Le Moigne, N.; Bergeret, A.; Wang, X.; Keller, P. Stimuli-Responsive Topological Change of Microstructured Surfaces and the Resultant Variations of Wetting Properties. *ACS Appl. Mater. Interfaces* **2013**, *5*, 7485−7491.
(14) Feng, C.L.; Zhang, Y.J.; Jin, J.; Song, Y.L.; Xie, L.Y.; Qu, G.R.; Jiang, L.; Zhu, D.B. Reversible Wettability of Photoresponsive Fluorine-Containing Azobenzene Polymer in Langmuir-Blodgett Films. *Langmuir* **2001**, *17*, 4593−4597.
(15) Lahann, J.; Mitragotri, S.; Tran, T.-N.; Kaido, H.; Sundaram, J.; Choi, I. S.; Hoffer, S.; Somorjai, G.A.; Langer, R. A Reversibly Switching Surface. *Science* **2003**, *299*, 371−374.
(16) Yakacki, C. M.; Shandas, R.; Lanning, C.; Rech, B.; Eckstein, A.; Gall, K. Unconstrained Recovery Characterization of Shape-Memory Polymer Networks for Cardiovascular Applications. *Biomaterials* **2007**, *28*, 2255−2263.
(17) Lendlein, A.; Langer, R. Biodegradable, Elastic Shape-Memory Polymers for Potential Biomedical Applications. *Science* **2002**, *296*, 1673−1676.
(18) Kim, D.-H.; Lipke, E. A.; Kim, P.; Cheong, R.; Thompson, S.; Delannoy, M.; Suh, K.-Y.; Tung, L.; Levchenko, A. Nanoscale Cues Regulate the Structure and Function of Macroscopic Cardiac Tissue Constructs. *Proc. Natl. Acad. Sci. U.S.A.* **2010**, *107*, 565−570.
(19) Lendlein, A.; Jiang, H.; Jünger, O.; Langer, R. Light-Induced Shape-Memory Polymers. *Nature* **2005**, *434*, 879−882.
(20) Idota, N.; Tsukahara, T.; Sato, K.; Okano, T.; Kitamori, T. The Use of Electron Beam Lithographic Graft-Polymerization on Thermoresponsive Polymers for Regulating the Directionality of Cell Attachment and Detachment. *Biomaterials* **2009**, *30*, 2095−2101.
(21) Xu, H.; Yu, C.; Wang, S.; Malyarchuk, V.; Xie, T.; Rogers, J.A. Deformable, Programmable, and Shape-Memorizing Micro-Optics. *Adv. Funct. Mater.* **2013**, *23*, 3299−3306.
(22) Le, D. M.; Kulangara, K.; Adler, A. F.; Leong, K. W.; Ashby, V. S. Dynamic Topographical Control of Mesenchymal Stem Cells by Culture on Responsive Poly(ε-Caprolactone) Surfaces. *Adv. Mater.* **2011**, *23*, 3278−3283.
(23) Zhou, J.; Turner, S. A.; Brosnan, S. M.; Li, Q.; Carrillo, J.-M. Y.; Gang, O.; Ashby, V. S.; Dobrynin, A. V.; Sheiko, S. S. Shapeshifting: Reversible Shape Memory in Semicrystalline Elastomers. *Macromolecules* **2014**, *47*, 1768−18775.
(24) Brosnan, S. M.; Brown, A .H.; Ashby, V. S. It Is the Outside that Counts: Chemical and Physical Control of Dynamic Surfaces. *J. Am. Chem. Soc.* **2013**, *135*, 3067−3072.
(25) Davis, K. A.; Burke, K. A.; Mather, P. T.; Henderson, J. H. Dynamic Cell Behavior on Shape Memory Polymer Substrates. *Biomaterials* **2011**, *32*, 2285−2293.
(26) Perry, J. L.; Herlihy, K. P.; Napier, M. E.; DeSimone, J. M. PRINT: A Novel Platform Toward Shape and Size Specific Nanoparticle Theranostics. *Acc. Chem. Res.* **2011**, *44*, 990−998.
(27) Buguin, A.; Li, M.-H.; Silberzan, P.; Ladoux, B.; Keller, P. Micro-Actuators: When Artificial Muscles Made of Nematic Liquid Crystal Elastomers Meet Soft Lithography. *J. Am. Chem. Soc.* **2006**, *128*, 1088−1089.
(28) van Oosten, C. L.; Bastiaansen, C. W. M.; Broer, D. J. Printed Artificial Cilia from Liquid-Crystal Network Actuators Modularly Driven by Light. *Nat. Mater.* **2009**, *8*, 677−682.
(29) Yang, H.; Ye, G.; Wang, X.; Keller, P. Micron-Sized Liquid Crystalline Elastomer Actuators. *Soft Matter* **2011**, *7*, 815−823.
(30) Lange, N. A. *Handbook of Chemistry*, 10th ed.; McGraw-Hill: New York, 1967.
(31) Behl, M.; Kratz, K.; Noechel, U.; Sauter, T.; Lendlein, A. Temperature-Memory Polymer Actuators. *Proc. Natl. Acad. Sci. U.S.A.* **2013**, *110*, 12555−12559.